

# Depletion of YTHDF1 Mitigates ox-LDL-Induced Human Coronary Endothelial Cell Dysfunction by Decreasing BACH1

Lina Fang<sup>1</sup>, Rui Yan<sup>1</sup>, Xiaozhen Chen<sup>1</sup>, Yunfu Yu<sup>1</sup>, Min Zheng<sup>1</sup>, Jifeng Yan<sup>1,\*</sup>

<sup>1</sup>Department of Cardiology, Central China Fuwai Hospital of Zhengzhou University, Fuwai Central China Cardiovascular Hospital and Central China Branch of National Center for Cardiovascular Diseases, 451464 Zhengzhou, Henan, China

\*Correspondence: [yanjifeng991@163.com](mailto:yanjifeng991@163.com) (Jifeng Yan)

Submitted: 26 December 2025 Revised: 16 March 2026 Accepted: 25 March 2026 Published: 20 April 2026

**Background:** Endothelial dysfunction is a pivotal contributor to coronary heart disease (CHD). The study aimed to elucidate the involvement of YT521-B homology domain 1 (YTHDF1) in mediating endothelial dysfunction triggered by oxidized low-density lipoprotein (ox-LDL) in human coronary artery endothelial cells (HCAECs).

**Methods:** Cell viability was evaluated using the Cell Counting Kit-8 (CCK-8) assay, while apoptotic status was determined by flow cytometric analysis. Cell migratory capacity was examined through a Transwell assay. The concentrations of pro-inflammatory cytokines (Tumor necrosis factor (TNF)- $\alpha$ , Interleukin (IL)-1 $\beta$ , and IL-18) together with the adhesion molecule VCAM-1 were measured using Enzyme-linked immunosorbent assay (ELISA). Intracellular Reactive oxygen species (ROS) production was assessed via DCFH-DA fluorescent staining. The N6-methyladenosine (m<sup>6</sup>A) modification level of BTB and CNC homology 1 (BACH1) was analyzed using Methylated RNA binding protein immunoprecipitation (MeRIP), and molecular interactions were further explored using RNA binding protein immunoprecipitation (RIP) assay.

**Results:** YTHDF1 expression was significantly increased in peripheral blood mononuclear cells (PBMCs) from CHD patients compared with healthy controls and in ox-LDL-treated HCAECs compared with untreated cells ( $p < 0.05$ ). YTHDF1 silencing significantly attenuated ox-LDL-induced endothelial injury, as evidenced by increased cell viability and migration and decreased apoptosis, inflammatory cytokine secretion, and ROS production (all  $p < 0.05$ ). Mechanistically, YTHDF1 promoted BACH1 mRNA translation in HCAECs in an m<sup>6</sup>A-dependent manner ( $p < 0.05$ ). Furthermore, BACH1 overexpression significantly reversed the protective effects of YTHDF1 knockdown on HCAEC survival and migration and restored ox-LDL-induced oxidative stress and inflammatory responses ( $p < 0.05$ ).

**Conclusion:** YTHDF1 promoted ox-LDL-induced HCAEC dysregulation by enhancing BACH1 mRNA translation in an m<sup>6</sup>A-dependent manner.

**Keywords:** coronary heart disease; endothelial dysfunction; YTHDF1; m<sup>6</sup>A; BACH1

## Introduction

Cardiovascular disease (CVD) continues to rank as the foremost cause of death on a global scale, accounting for nearly 31% of all recorded mortalities worldwide, and its prevalence is steadily increasing [1]. Coronary heart disease (CHD) is the most prevalent form of CVD, mainly caused by atherosclerosis (AS) [2]. Although significant progress has been made in the treatment strategies for CHD at present, the mortality rate of CHD is still very high [3]. Therefore, there is an urgent need to develop new diagnostic and therapeutic strategies for CHD, and exploring effective intervention targets and regulatory mechanisms involved in the pathophysiological processes is essential to achieving this goal.

N6-methyladenosine (m<sup>6</sup>A) modification, as an apparent RNA modification, is a key player in CHD progres-

sion [4]. m<sup>6</sup>A modification is regulated by m<sup>6</sup>A methyltransferase, m<sup>6</sup>A binding protein, and m<sup>6</sup>A demethylase [5]. Studies have demonstrated that m<sup>6</sup>A-related regulatory factors and the mediated RNA methylation modifications are key players in CHD development [4,6]. Specifically, YT521-B homology domain 1 (YTHDF1), as a key reader in m<sup>6</sup>A methylation modification, can maintain RNA stability by binding to m<sup>6</sup>A-modified mRNA, thereby regulating various physiological and pathological activities [7]. YTHDF1 has diagnostic significance in the diagnosis and subtype classification of CHD [4,8]. In addition, a previous publication showed that YTHDF1 could aggravate AS by activating NLRP3 inflammasome through promoting UCHL5 mRNA stability [9], suggesting that YTHDF1 might be a key regulator in CHD progression. However, the underlying mechanism by which YTHDF1 regulates CHD development remains unclear.

The vascular endothelium, a monolayer of cells lining the blood vessel lumen, is indispensable for the maintenance of physiological vascular function [10]. Increasing evidence has established endothelial dysfunction as a hallmark pathological feature of a broad spectrum of vascular diseases, including CHD [11–13]. While accumulating evidence has linked the m<sup>6</sup>A reader protein YTHDF1 to endothelial cell function regulation [14–17], its specific role in CHD-associated endothelial dysfunction remains unexplored. To address this knowledge gap, we systematically examined the role of YTHDF1 in endothelial dysfunction triggered by oxidized low-density lipoprotein (ox-LDL) in human coronary artery endothelial cells (HCAECs). Central to our study is BTB and CNC homology 1 (BACH1), a transcriptional regulator recently implicated in cardiovascular pathophysiology through dual mechanisms: (1) suppressing the nuclear factor erythroid 2-related factor 2/antioxidant response element (Nrf2/ARE) antioxidant pathway to exacerbate oxidative stress in endothelial cells [18], and (2) activating nuclear factor kappa B (NF- $\kappa$ B) signaling to promote proinflammatory cytokine secretion (tumor necrosis factor- $\alpha$ , TNF- $\alpha$ ; interleukin-6, IL-6) and accelerate atherosclerosis [19]. Furthermore, integrated bioinformatics analyses using RM2Target and Sequence-based RNA Adenosine Methylation Site Predictor (SRAMP) databases predicted m<sup>6</sup>A modification sites on BACH1 mRNA, while starBase data revealed potential YTHDF1-BACH1 interactions. These findings collectively suggest BACH1 serves as a critical nexus connecting oxidative stress, inflammation, and endothelial dysfunction in CHD pathogenesis. Therefore, we hypothesized that YTHDF1 might regulate endothelial inflammation, oxidative stress and dysfunction through m<sup>6</sup>A-dependent modulation of BACH1.

## Methods

### *Clinical Sample Collection*

The peripheral blood samples (5 mL per subject) were collected from 32 CHD patients and 32 healthy volunteers from Fuwai Central China Cardiovascular Hospital (Cardiac Center of Henan Province People's Hospital) between March 2025 and June 2025. All CHD patients were diagnosed by diagnostic coronary angiography. All participants were over 18 years old, had no history of cardiovascular surgery or major diseases, including cardiomyopathy, congenital heart disease, severe liver and kidney disease, systemic autoimmune diseases, or malignant tumors. Baseline demographic and clinical variables, including age, sex, body mass index (BMI), lipid profiles, hypertension, and diabetes, were systematically collected and are presented in Table 1. Blood samples were obtained in ethylenediaminetetraacetic acid-containing tubes and rapidly processed ( $\leq 30$  min) to minimize degradation. This investigation received ethical approval from the Institutional Re-

view Board of Fuwai Central China Cardiovascular Hospital (Approval No. 2025-102) and followed the Declaration of Helsinki. Written informed consent was obtained from all participants prior to sample collection. For clinical correlation analysis between YTHDF1 expression and CHD, peripheral blood mononuclear cells (PBMCs) from patients with CHD and matched healthy controls were prepared via Ficoll-Paque PLUS (GE Healthcare, IL, USA) gradient separation. In brief, whole blood was diluted 1:1 in PBS, carefully layered over Ficoll, and centrifuged at 400  $\times$ g for 30 min at 20  $^{\circ}$ C without deceleration. Cells at the plasma-Ficoll boundary were collected, washed twice in PBS, and reconstituted in RPMI-1640 medium (11875085, Gibco, MD, USA). Sample handling was completed within 4 h of blood draw to maintain PBMC viability.

For transcriptome profiling, PBMC-derived RNA was isolated using Trizol Reagent (15596026CN, Invitrogen, CA, USA) according to a standard chloroform-isopropanol extraction procedure with ethanol washing. RNA purity and yield were assessed using NanoDrop analysis, and only samples with A260/A280 values exceeding 1.8 were used. Protein extraction was performed by lysing PBMCs in pre-cooled RIPA buffer (P0013E, Beyotime, Shanghai, China) supplemented with 1% protease inhibitor cocktail (Roche, Basel, Switzerland) for 30 min on ice, followed by centrifugation at 14,000  $\times$ g for 20 min at 4  $^{\circ}$ C. Protein concentration was quantified using the BCA assay (A65453, ThermoFisher Scientific, MA, USA).

### *Cell Culture and Stimulation*

HCAECs were obtained from Lonza (CC-2585, Basel, Switzerland) and cultured in endothelial growth medium (C-22011, Promocell, Germany) at 37  $^{\circ}$ C with 5% CO<sub>2</sub>. HCAECs had been authenticated by short tandem repeat (STR) identification and confirmed negative for mycoplasma. HCAECs were exposed to 100  $\mu$ g/mL ox-LDL (Sigma-Aldrich, MO, USA) for 48 h as previously described [20].

### *Reverse Transcription Quantitative Polymerase Chain Reaction (RT-qPCR)*

Total RNA preparation was performed with TRIzol (Invitrogen), and reverse transcription was subsequently conducted using a standard cDNA synthesis kit (4374966, Invitrogen). SYBR-based quantitative real-time PCR (S33102, Applied Biosystems, CA, USA) was applied for gene expression analysis. GAPDH was used as an internal reference, and relative expression levels were derived using the 2<sup>- $\Delta\Delta$ CT</sup> method. Primer sequences are shown in the 5'-3' direction.

YTHDF1 (F): CGTGGACACCCAGAGAACAA;

YTHDF1 (R): TAGCTGGACAGGTAGGGGTC.

Oxidized Low-Density Lipoprotein Receptor 1 (OLR1) (F): TGGCATGCAATTATCCCAG;

OLR1 (R): CTAAATAAGTGGGGCATCAAAGG;

**Table 1. Anthropometric and laboratory measurements of the study population.**

Parameter	Control (N = 32)	CHD (N = 32)	$\chi^2/t$	<i>p</i>
Gender (male/female)	17/15	14/18	0.563	0.453
Age (years)	54.47 ± 2.65	55.81 ± 3.66	-1.682	0.098
Body mass index (kg/m <sup>2</sup> )	25.54 ± 0.97	26.19 ± 1.39	-2.152	0.035
Systolic blood pressure (mmHg)	129.6 ± 2.5	130.2 ± 3.1	-0.938	0.352
Diastolic blood pressure (mmHg)	82.00 ± 1.40	82.52 ± 1.66	-1.354	0.181
Fasting blood sugar (mg/dL)	91.93 ± 1.55	92.38 ± 1.59	-1.146	0.256
LDL-Cholesterol (mg/dL)	74.58 ± 2.47	75.01 ± 2.03	-0.753	0.455
HDL-Cholesterol (mg/dL)	44.11 ± 0.54	38.14 ± 1.24	24.918	<0.0001
Triglycerides (mg/dL)	133.2 ± 4.4	135.6 ± 5.4	-1.988	0.051
Total Cholesterol (mg/dL)	137.0 ± 3.7	138.0 ± 3.2	-1.092	0.279

CHD, Coronary heart disease; LDL, low-density lipoprotein; HDL, high-density lipoprotein.

BACH1 (F): TGCACAAGCTTACTCCAGAAC;  
 BACH1 (R): TTCTGCTTTGTCTCACCCAG;  
 GAPDH (F): AAGATCATCAGCAATGCCTCC;  
 GAPDH (R): AGGTTTTTCTAGACGGCAGG.

### Western Blot Analysis

Proteins were extracted from cultured cells with RIPA lysis buffer (P0013B, Beyotime, Shanghai, China) and subsequently quantified using a BCA assay kit (A65453, ThermoFisher Scientific, Waltham, MA, USA). Equal amounts of protein were separated on 10% SDS-PAGE gels and subsequently transferred onto PVDF membranes (Millipore, Billerica, MA, USA). After membrane blocking, primary antibodies were applied for overnight incubation at 4 °C, including YTHDF1 (1:1000, ab220162, Abcam, Cambridge, UK), BACH1 (1:10,000, ab300130, Abcam, Cambridge, UK), Lectin-like ox-LDL receptor-1 (LOX-1, 1:1000, ab214427, Abcam, Cambridge, UK), Caspase-3 (1:5000, ab32351, Abcam, Cambridge, UK), Cleaved-caspase-3 (1:1000, ab32042, Abcam, Cambridge, UK), endothelial nitric oxide synthase (eNOS, 1:1000, ab252439, Abcam, Cambridge, UK), phosphorylated endothelial nitric oxide synthase (p-eNOS, S1177) (1:1000, ab215717, Abcam, Cambridge, UK), and GAPDH (1:5000, ab8245, Abcam, Cambridge, UK). After washing with PBS-T, membranes were incubated for 1 h at room temperature with horseradish peroxidase (HRP)-conjugated goat anti-rabbit IgG (1:10,000; ab7090, Abcam, Cambridge, UK) or HRP-conjugated goat anti-mouse IgG (1:10,000; ab6789, Abcam, Cambridge, UK) according to the host species of the primary antibody. Protein bands were visualized using an enhanced chemiluminescence detection kit (ECL; PK10001, Beyotime, Shanghai, China) and imaged using a chemiluminescence imaging system (Bio-Rad, Hercules, CA, USA).

### Cell Transfection

GenePharma (Shanghai, China) provided all genetic manipulation constructs, including short hairpin RNA targeting YTHDF1 (sh-YTHDF1#1 and sh-YTHDF1#2), sh-

BACH1, pcDNA3.1-YTHDF1, pcDNA3.1-BACH1, and sh-NC. The empty pcDNA3.1 vector (GM-1013P001, Genomeditech, Shanghai, China) was used as the negative control plasmid. Cellular transfection was conducted using Lipofectamine 3000 (Invitrogen, Carlsbad, CA, USA) following the manufacturer's instructions. HCAECs were maintained in antibiotic-free 6-well plates at an initial density of  $2 \times 10^5$  cells per well until 70–80% confluence. For complex formation, 2 µg plasmid DNA or 50 pmol shRNA was diluted in 125 µL Opti-MEM (Gibco, Grand Island, NY, USA) and incubated with Lipofectamine 3000 for 15 min at ambient temperature. Cells were then incubated with the transfection mixture for 6 h, after which fresh complete medium was added for an additional 48 h. RT-qPCR analysis was used to confirm transfection efficiency. The shRNA targeting sequence was provided in **Supplementary Table 1**. The complete insertion sequences of pcDNA3.1-YTHDF1 and pcDNA3.1-BACH1 are provided in the **Supplementary Material 1**.

HCAECs were treated with 10 µM 3-deazaadenosine (DAA; D8296, Sigma-Aldrich, St. Louis, MO, USA) for 24 h following transfection with pcDNA3.1-YTHDF1.

### Cell Counting Kit-8 (CCK-8) Assay

After completion of the indicated transfection procedures, HCAECs, including shNC-, shYTHDF1-, and shYTHDF1+pcDNA3.1-BACH1-transfected cells, were plated into 96-well culture plates at  $5 \times 10^3$  cells per well. Following an overnight attachment period, cells were exposed to 100 µg/mL ox-LDL for 0, 24, 48, or 72 h. At each scheduled time point, cells were treated with 10 µL of CCK-8 solution (E606335-0100, Sangon, Shanghai, China) followed by incubation for 3 h under standard culture conditions (37 °C, 5% CO<sub>2</sub>). Cell viability was subsequently evaluated by measuring the optical density at 450 nm using a microplate reader (BioTek, Winooski, VT, USA).

### Cell Apoptosis Assay

After 48 h of transfection (shNC, shYTHDF1, or shYTHDF1 co-transfected with pcDNA3.1-BACH1),

HCAECs were treated with 100  $\mu\text{g}/\text{mL}$  ox-LDL for an additional 48 h. Apoptosis was evaluated using an Annexin V-FITC/propidium iodide (PI) apoptosis detection kit (556547, BD Biosciences, San Jose, CA, USA) according to the manufacturer's instructions. Briefly, harvested cells were resuspended in 500  $\mu\text{L}$   $1\times$  Annexin binding buffer (BD Biosciences, San Jose, CA, USA), followed by incubation with Annexin V-FITC (10  $\mu\text{L}$ ) and PI (5  $\mu\text{L}$ ) for 10 min at room temperature in the dark. Apoptotic cells were immediately analyzed using a BD FACSCanto II flow cytometer (BD Biosciences, San Jose, CA, USA), and data were processed using FlowJo software (version 10.8, BD Biosciences, Ashland, OR, USA).

#### Transwell Assay

HCAECs were subjected to transfection with shNC, shYTHDF1, or shYTHDF1 plus pcDNA3.1-BACH1 for 48 h, and subsequently challenged with 100  $\mu\text{g}/\text{mL}$  ox-LDL for another 48 h. Cell migratory capacity was determined using a Transwell system (24-well, 8.0  $\mu\text{m}$  pore membranes, Corning, Corning, NY, USA). After a 6 h serum-starvation step, cells were collected and resuspended in serum-free medium. For the migration assay, approximately  $1\times 10^4$  cells suspended in 200  $\mu\text{L}$  were added to the upper chamber, whereas 500  $\mu\text{L}$  of complete medium was seeded into the lower chamber. Following 24 h incubation, cells remaining on the upper surface were wiped off with cotton swabs, and cells on the underside were fixed with 4% paraformaldehyde (P0099, Beyotime, Shanghai, China) and stained with 0.1% crystal violet (C0121, Beyotime, Shanghai, China). Images were captured at  $200\times$  using an Olympus microscope (Tokyo, Japan). For each transwell membrane, five non-overlapping fields (center and four corners) were randomly photographed. Each experimental group included three biological replicates, and the assay was repeated three times independently. Migrated cells were quantified manually using ImageJ software (version 1.53, National Institutes of Health, Bethesda, MD, USA).

#### Reactive Oxygen Species (ROS) Detection

A fluorescent probe, DCFH-DA reagent (2044-85-1, Sigma-Aldrich, St. Louis, MO, USA), was available for detecting cellular ROS accumulation. In short, HCAECs ( $1\times 10^5$  cells/well) after indicated treatment were stained with 10  $\mu\text{M}$  DCFH-DA solution in complete medium for 30 min. After samples were washed, ROS-associated fluorescence signals were rapidly visualized and recorded using a fluorescence microscope (Olympus, Tokyo, Japan) at  $200\times$  magnification. For each experimental group, four random and non-overlapping fields per well were captured. Each condition included three biological replicates (wells), and the experiment was repeated three times independently. Fluorescence intensity was quantified using ImageJ software (version 1.53, National Institutes of Health, Bethesda,

MD, USA). For statistical analysis, three regions were randomly selected per image (excluding cell-free areas), and the average fluorescence intensity was measured. Background signal from blank wells (without cells) was subtracted to obtain the final relative ROS fluorescence intensity.

#### Enzyme-Linked Immunosorbent Assay (ELISA)

HCAECs were genetically modified with shNC, shYTHDF1, or shYTHDF1 combined with pcDNA3.1-BACH1 and cultured for 48 h, followed by exposure to 100  $\mu\text{g}/\text{mL}$  ox-LDL for 48 h. The concentrations of TNF- $\alpha$ , IL-1 $\beta$ , IL-18, VCAM-1, and NO were determined via enzyme-linked immunosorbent assays using reagents from Abcam (ab181421, ab214025, ab215539, ab223591, ab65328; Abcam, Cambridge, UK).

#### Measurement of Malondialdehyde (MDA) and Glutathione (GSH) Levels

Intracellular glutathione (GSH) content and malondialdehyde (MDA) levels were quantitatively determined using the GSH assay kit (A006-2-1, Nanjing Jiancheng, China) and the MDA assay kit (A003-1-2, Nanjing Jiancheng, China), strictly following the manufacturers' protocols.

#### RNA Binding Protein Immunoprecipitation (RIP) Assay

HCAECs were processed using RIP buffer for cell lysis, after which the lysates were systematically harvested. YTHDF1 antibody (1:30, ab220162, Abcam, Cambridge, UK) or control anti-immunoglobulin G (IgG) antibody (1:100, ab109489, Abcam, Cambridge, UK) was pre-bound to pre-cleaned magnetic beads (P2102, Beyotime, Shanghai, China) by overnight incubation at 4  $^{\circ}\text{C}$ . After formation of the antibody-bead complexes, these conjugates were allowed to interact with cellular lysates for 4 h, after which total RNA was extracted using Trizol reagent (Thermo Fisher Scientific, Waltham, MA, USA), and the immunoenriched RNA fraction was subsequently quantified by RT-qPCR.

#### Methylated RNA Immunoprecipitation (MeRIP)

Potential m<sup>6</sup>A modification sites within the BACH1 mRNA were first screened using the SRAMP database (<http://www.cuilab.cn/sramp>). Total RNA isolated from HCAECs by TRIzol extraction (R0016, Beyotime, Shanghai, China) was subjected to mRNA purification and chemically fragmented into approximately 100-nt fragments. An m<sup>6</sup>A-specific antibody (1:500, ab151230, Abcam, Cambridge, UK) or control IgG (1:100, ab109489, Abcam, Cambridge, UK) was pre-conjugated to protein A/G magnetic beads (10006D, Thermo Fisher Scientific, Waltham, MA, USA) in IP buffer (50 mM Tris-HCl, pH 7.4; 150 mM NaCl; 1% NP-40) for 1 h. The antibody-coated beads were subsequently incubated with fragmented mRNA at 4  $^{\circ}\text{C}$  for

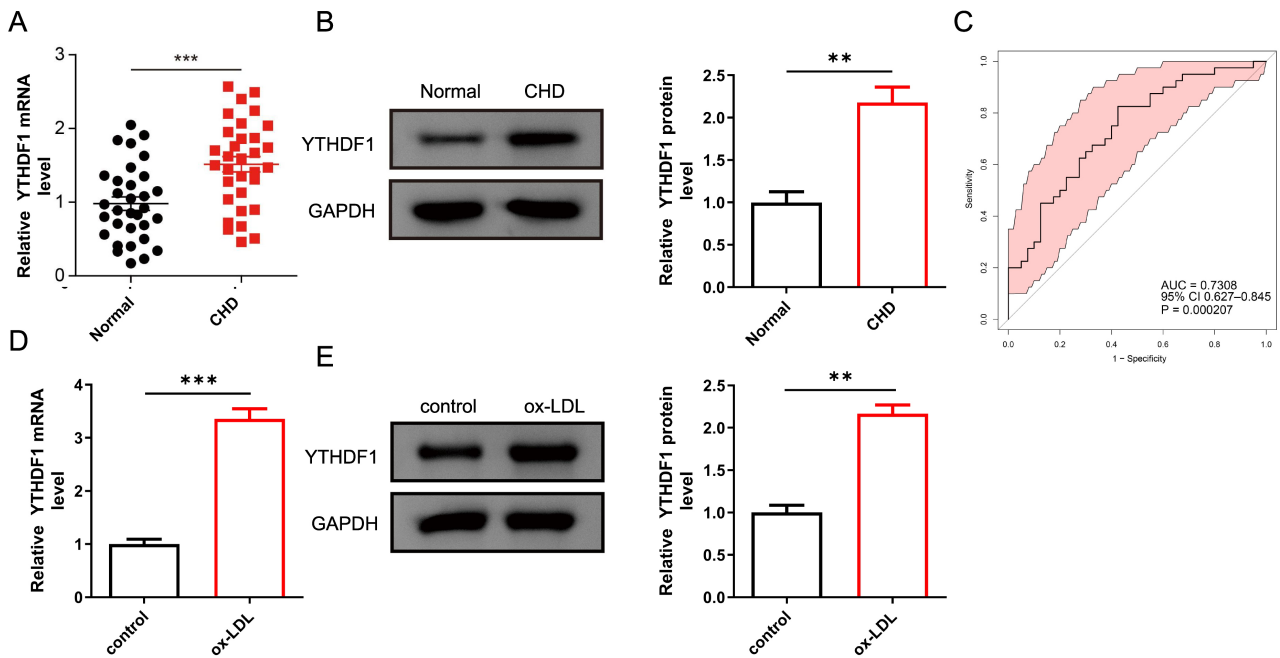


**Fig. 1. YTHDF1 was highly expressed in the blood samples of CHD patients and ox-LDL-treated HCAECs.** Blood specimens were obtained from 32 patients diagnosed with CHD and 32 matched healthy individuals, followed by peripheral blood mononuclear cell (PBMC) isolation. (A,B) YTHDF1 expression at both transcript and protein levels in PBMCs was quantified using RT-qPCR and Western blot analysis, respectively. (C) Receiver operating characteristic (ROC) curve analysis was applied to assess the diagnostic value of plasma YTHDF1 in CHD. (D,E) Human coronary artery endothelial cells (HCAECs) were exposed to 100  $\mu\text{g}/\text{mL}$  ox-LDL for 48 h, after which cellular YTHDF1 mRNA and protein expression were evaluated. Data are presented as mean  $\pm$  SD ( $n = 3$ ).  $**p < 0.01$ ,  $***p < 0.001$ . YTHDF1, YT521-B homology domain 1; CHD, Coronary heart disease; ox-LDL, Oxidized low-density lipoprotein; PBMCs, peripheral blood mononuclear cells; RT-qPCR, reverse transcription quantitative polymerase chain reaction; ROC, receiver operating characteristic; SD, standard deviation.

4 h, followed by washing and RT-qPCR-based quantification of the enriched RNA.

#### Data Analysis

All *in vitro* experiments were conducted with three biological replicates ( $n = 3$ ). For each biological replicate, three technical replicates were performed. Statistical analyses were performed using SPSS (version 19.0, IBM Corp., Armonk, NY, USA), with data expressed as mean  $\pm$  standard deviation (SD). Categorical variables were assessed via the  $\chi^2$  test, while comparisons between two continuous-variable groups were performed using Student's *t*-test. One-way analysis of variance (ANOVA) followed by Tukey's post hoc test was applied for analyses involving more than two groups. Moreover, receiver operating characteristic (ROC) curve analysis was conducted to assess the diagnostic capability of plasma YTHDF1 in CHD. Differences were considered statistically significant at  $p < 0.05$ .

## Results

### *YTHDF1 Was Highly Expressed in CHD Patients and ox-LDL-Treated HCAECs*

This study included 64 participants, comprising 32 patients with CHD and 32 matched healthy controls, whose baseline clinical characteristics are shown in Table 1. Compared with the control group, patients with CHD had higher BMI and lower high-density lipoprotein cholesterol (HDL-C) levels. Next, the expression level of YTHDF1 in CHD and normal subjects was determined. As shown in Fig. 1A,B, YTHDF1 expression was elevated in PBMCs of CHD patients compared with that in healthy controls. Using HDL-C as a covariate, the results showed that YTHDF1 expression in the CHD group was still significantly higher than that in the control group (Supplementary Table 2;  $p = 0.003$ ). The diagnostic potential of plasma YTHDF1 for CHD was evaluated by ROC curve analysis, and the data showed that the area under the curve (AUC) was 0.7308 (95% CI: 0.627–0.845;  $p < 0.001$ ) (Fig. 1C), indicating that YTHDF1 had great diagnostic potential for CHD. Next, HCAECs were exposed to ox-LDL to establish an *in vitro* model of endothelial dysfunction, a key patholog-

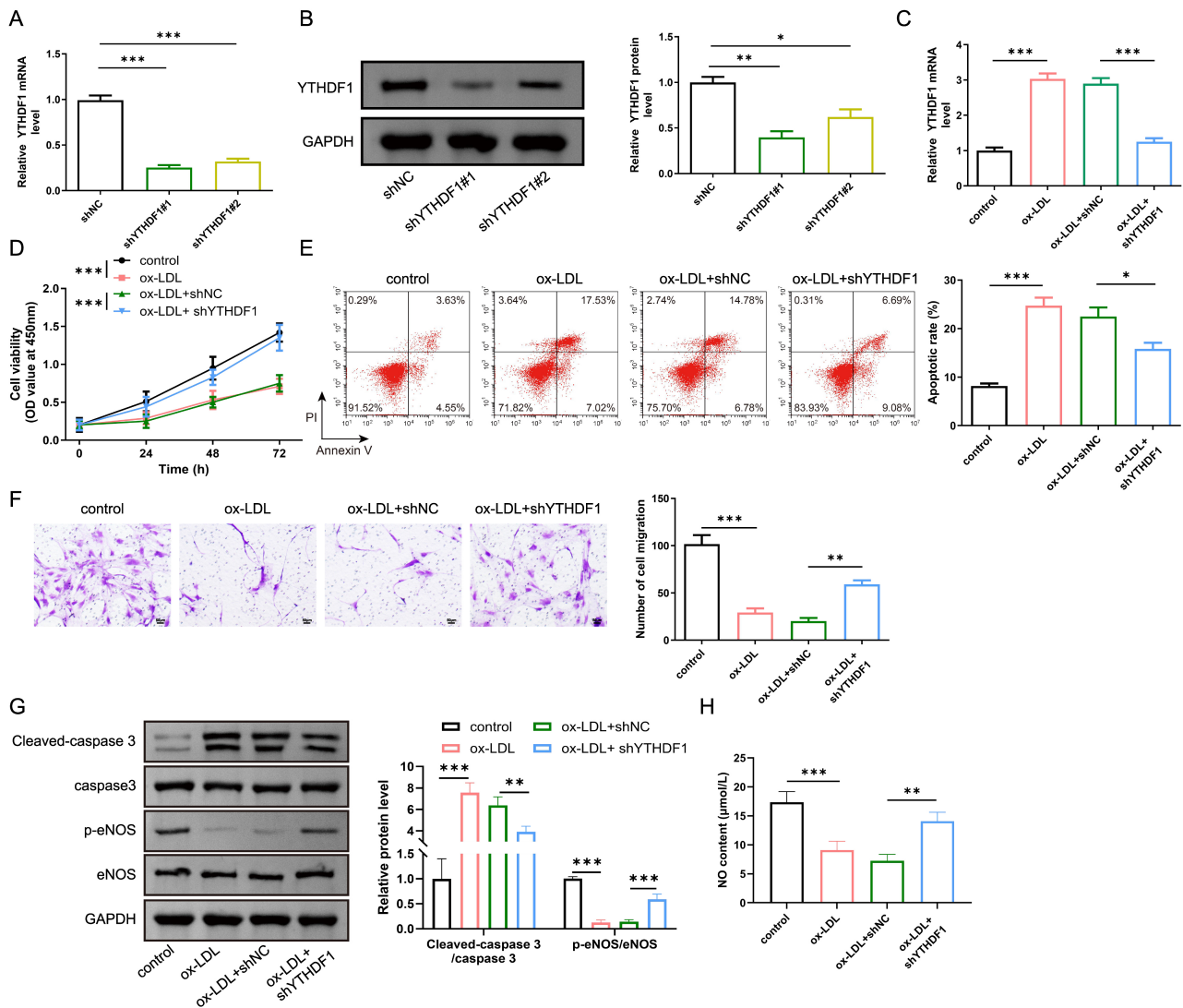


**Fig. 2. YTHDF1 suppression alleviated ox-LDL-induced impairment of HCAEC survival and migration.** (A,B) The mRNA and protein levels of YTHDF1 in HCAECs after sh-NC, sh-YTHDF1#1 or sh-YTHDF1#2 transfection were determined by RT-qPCR and Western blot analysis, respectively. HCAECs were transfected with sh-NC or sh-YTHDF1 for 48 h and then exposed to 100 μg/mL ox-LDL for 48 h. (C) RT-qPCR was employed to quantify the relative transcript levels of YTHDF1. (D) Cellular viability was determined using the CCK-8 assay. (E) Apoptotic rates were analyzed by flow cytometry. (F) Cell migratory capacity was examined via a Transwell assay. Scale bar = 50 μm. (G) Protein expression levels of Caspase-3, Cleaved-caspase-3, eNOS, and p-eNOS (S1177) were assessed using Western blotting. (H) NO generation in cells was measured using ELISA. Data are presented as mean ± SD (n = 3). \**p* < 0.05, \*\**p* < 0.01, \*\*\**p* < 0.001. sh-NC, short hairpin RNA negative control; CCK-8, Cell Counting Kit-8; eNOS, endothelial nitric oxide synthase; p-eNOS, phosphorylated endothelial nitric oxide synthase; ELISA, Enzyme-linked immunosorbent assay; NO, Nitric oxide.

ical feature of CHD. It suggested that ox-LDL stimulation markedly elevated YTHDF1 expression level in HCAECs (Fig. 1D,E). Collectively, YTHDF1 was significantly up-regulated in CHD.

#### *YTHDF1 Suppression Alleviated ox-LDL-Induced Impairment of HCAEC Survival and Migration*

To further study the role of YTHDF1 in regulating HCAEC function *in vitro*, shRNAs against YTHDF1 were transfected into HCAECs. As shown in Fig. 2A,B, both sh-

YTHDF1#1 and sh-YTHDF1#2 transfection significantly reduced YTHDF1 expression level in HCAECs (*p* < 0.05). In addition, sh-YTHDF1#1 exhibited higher knockdown efficiency compared to sh-YTHDF1#2 (Fig. 2A,B). In the subsequent experiments, sh-YTHDF1#1 was used. It was observed that sh-YTHDF1 transfection ameliorated ox-LDL-induced increase in YTHDF1 expression in HCAECs (Fig. 2C; *p* < 0.05). In addition, HCAEC viability was impaired by ox-LDL, while YTHDF1 silencing reversed this effect (Fig. 2D; *p* < 0.05). Furthermore, ox-LDL treatment

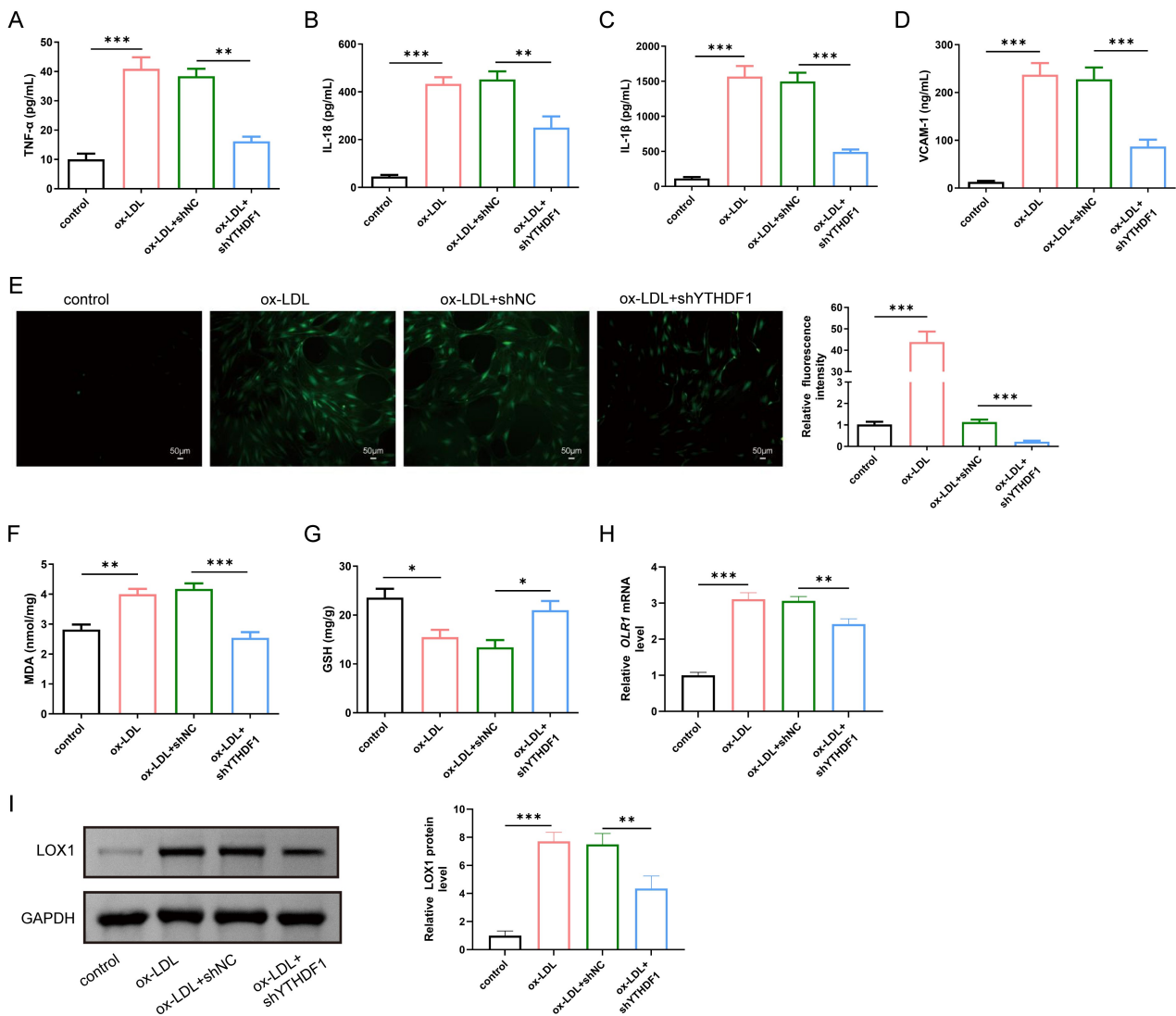


**Fig. 3. Loss of YTHDF1 overturned ox-LDL-induced inflammatory responses and oxidative stress in HCAECs.** HCAECs were first subjected to transfection with sh-NC or sh-YTHDF1 for 48 h, followed by subsequent stimulation with 100  $\mu$ g/mL ox-LDL for an additional 48 h. ELISA assays were employed to quantify the secretion levels of TNF- $\alpha$ , IL-18, IL-1 $\beta$ , and VCAM-1 in HCAECs (A–D). Intracellular ROS accumulation was visualized and evaluated using DCFH-DA staining (E). Oxidative stress-related indicators, including MDA and GSH levels, were assessed using corresponding commercial kits (F,G). *OLR1* mRNA expression was measured by RT-qPCR, while LOX-1 protein expression was evaluated by Western blot analysis (H,I). All quantitative results are expressed as mean  $\pm$  SD ( $n = 3$ ). \* $p < 0.05$ , \*\* $p < 0.01$ , \*\*\* $p < 0.001$ . TNF, Tumor necrosis factor; IL, Interleukin; VCAM-1, vascular cell adhesion molecule-1; DCFH-DA, 2',7'-dichlorodihydrofluorescein diacetate; MDA, Malondialdehyde; GSH, Glutathione; *OLR1*, Oxidized Low-Density Lipoprotein Receptor 1; LOX-1, Lectin-like oxidized low-density lipoprotein receptor-1.

markedly facilitated HCAEC apoptosis, which was mitigated by YTHDF1 knockdown (Fig. 2E;  $p < 0.05$ ). It also indicated that HCAEC migration was impaired by ox-LDL treatment, whereas this change was abolished by YTHDF1 silencing (Fig. 2F;  $p < 0.05$ ). We also performed Western blot analysis for Cleaved Caspase-3 on protein extracts from HCAECs, and the results clearly showed that ox-LDL treatment markedly increased Cleaved-caspase-3/caspase-3 ratio, and this increase was significantly attenuated by

YTHDF1 knockdown (Fig. 2G;  $p < 0.05$ ). It was also observed that ox-LDL treatment significantly reduced eNOS phosphorylation (at Ser1177) and nitric oxide (NO) levels in HCAECs, while YTHDF1 knockdown restored eNOS phosphorylation and NO production (Fig. 2G,H;  $p < 0.05$ ). All these results suggested that YTHDF1 knockdown enhanced cell viability and migration but alleviated apoptosis in ox-LDL-induced HCAECs.

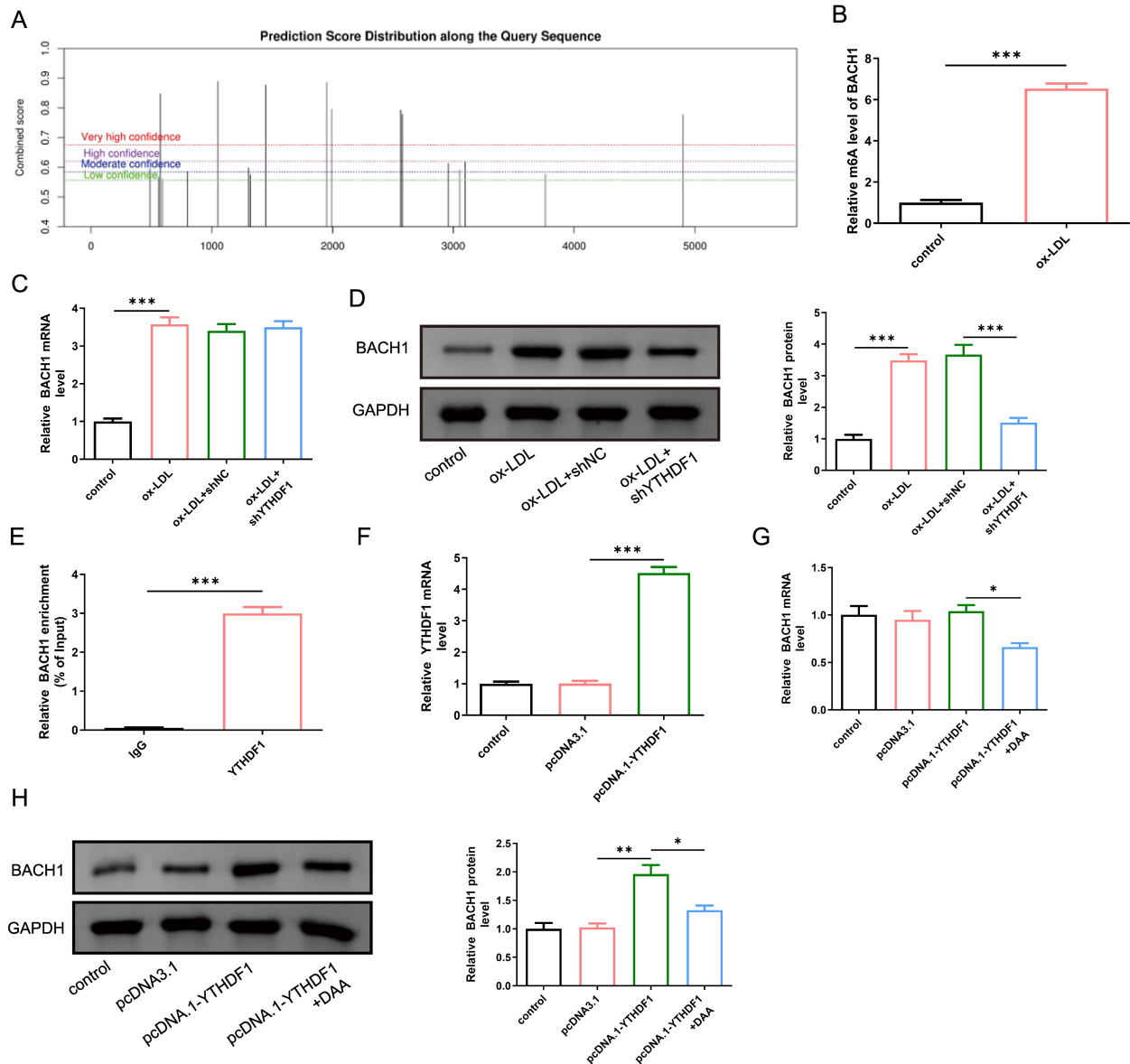


**Fig. 4. BACH1 was an m<sup>6</sup>A regulatory target of YTHDF1 in HCAECs.** (A) The m<sup>6</sup>A modification sites in BACH1 mRNA were predicted using the SRAMP database (<http://www.cuilab.cn/sramp>). (B) The relative m<sup>6</sup>A enrichment of BACH1 transcripts in HCAECs under ox-LDL challenge was analyzed by MeRIP assay. (C,D) Following sh-NC or sh-YTHDF1 transfection and 48 h ox-LDL treatment, BACH1 expression was evaluated at the mRNA and protein levels using RT-qPCR and Western blotting. (E) RIP assay was conducted to determine whether YTHDF1 directly associates with BACH1 mRNA. (F) Alterations in YTHDF1 mRNA expression after plasmid transfection were quantified via RT-qPCR. (G,H) The combined impact of YTHDF1 overexpression and DAA intervention on BACH1 expression was assessed using RT-qPCR and Western blot analyses. Data are presented as mean  $\pm$  SD (n = 3). \* $p$  < 0.05, \*\* $p$  < 0.01, \*\*\* $p$  < 0.001. BACH1, BTB and CNC homology 1; m<sup>6</sup>A, N6-methyladenosine; SRAMP, sequence-based RNA adenosine methylation site predictor; MeRIP, methylated RNA immunoprecipitation; RIP, RNA binding protein immunoprecipitation; DAA, 3-deazaadenosine.

### *Loss of YTHDF1 Overturned ox-LDL-Induced Inflammatory Responses and Oxidative Stress in HCAECs*

Endothelial oxidative stress and inflammation are important pathological features of CHD [21]. Our study focused on investigating the regulatory function of YTHDF1 in endothelial oxidative stress and inflammation. Our re-

sults displayed that exposure to ox-LDL markedly upregulated the release of inflammatory cytokines, including TNF- $\alpha$ , IL-18, IL-1 $\beta$ , and VCAM-1, in HCAECs, whereas this upregulation was substantially attenuated upon YTHDF1 knockdown (Fig. 3A–D;  $p$  < 0.05). Additionally, ox-LDL treatment led to a significant increase in ROS and MDA levels, accompanied by a decrease in GSH levels in HCAECs

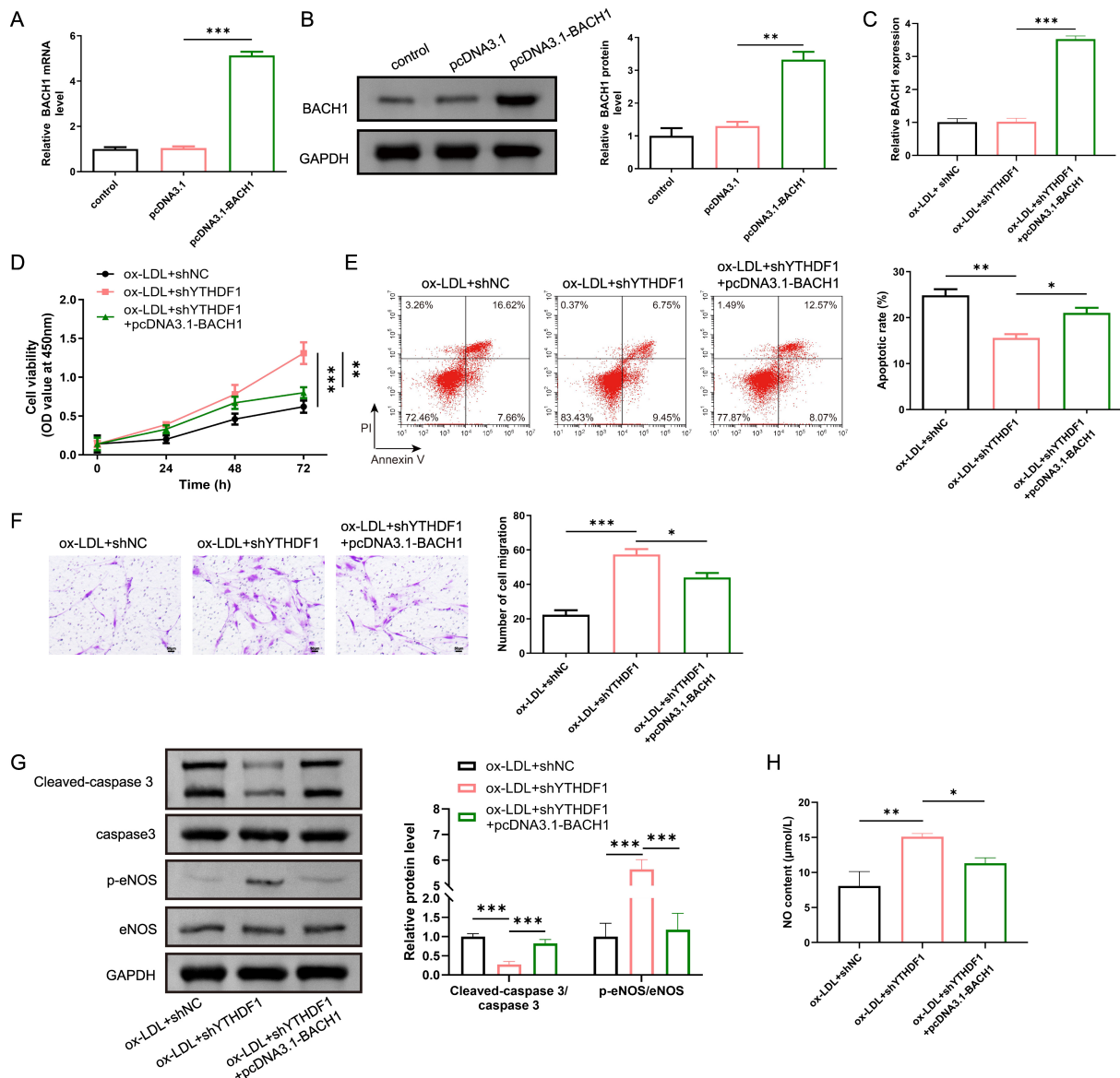


**Fig. 5. Overexpression of BACH1 reversed the protective roles of YTHDF1 silencing on HCAECs survival and migration.** (A) RT-qPCR analysis was used to determine BACH1 mRNA levels in HCAECs transfected with either pcDNA3.1 or pcDNA3.1-BACH1. After 48 h of co-transfection with pcDNA3.1-BACH1 and sh-YTHDF1, cells were exposed to ox-LDL for another 48 h. (B) BACH1 protein expression was examined by Western blotting. (C) Changes in BACH1 mRNA abundance were further verified using RT-qPCR. (D) Cell viability was evaluated through the CCK-8 assay. (E) Apoptosis was quantified by flow cytometry. (F) Cell migratory behavior was investigated using a Transwell system. Scale bar = 50  $\mu$ m. (G) Western blotting was performed to detect Caspase-3, Cleaved-caspase-3, eNOS, and phosphorylated eNOS (S1177). (H) NO levels were quantified using ELISA. All values are expressed as mean  $\pm$  SD (n = 3). \* $p$  < 0.05, \*\* $p$  < 0.01, \*\*\* $p$  < 0.001.

( $p$  < 0.05). Importantly, these oxidative stress-related changes were also reversed by YTHDF1 silencing (Fig. 3E–G;  $p$  < 0.05). LOX-1 is highly enriched in endothelial cells and serves as the key receptor for ox-LDL. Their interaction plays a crucial role in promoting endothelial dysfunction and cardiovascular diseases [22,23]. Furthermore, numerous reports have clearly established LOX-1's important function in mediating inflammatory responses and oxidative stress during cardiovascular disease pathogenesis

[24,25]. As shown in Fig. 3H,I, LOX-1 expression was significantly elevated in ox-LDL-treated HCAECs, while this increase was substantially attenuated following YTHDF1 knockdown ( $p$  < 0.05). Taken together, YTHDF1 knockdown possibly reduced ox-LDL-induced inflammatory responses and oxidative stress in HCAECs by inhibiting LOX-1 expression.

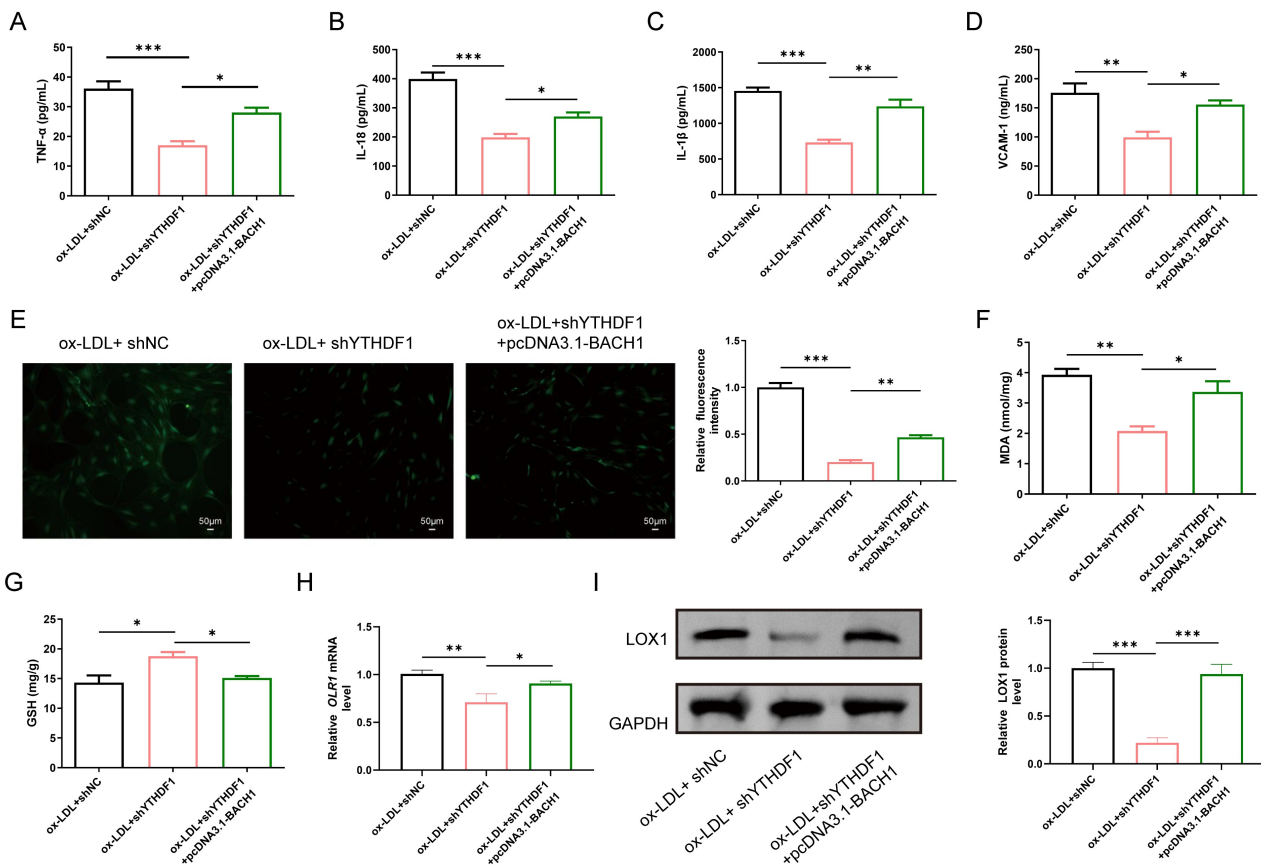


**Fig. 6. BACH1 overexpression diminished the promoting roles of YTHDF1 knockdown on ox-LDL-triggered oxidative stress and inflammation in HCAECs.** HCAECs were simultaneously subjected to pcDNA3.1-BACH1 overexpression and sh-YTHDF1 silencing for 48 h, followed by an additional 48-h exposure to ox-LDL. Cellular secretion of TNF- $\alpha$ , IL-18, IL-1 $\beta$ , and VCAM-1 (A–D) was quantified using ELISA assays. Intracellular ROS accumulation was evaluated by DCFH-DA fluorescence staining (E). Levels of oxidative stress markers, including MDA and GSH, were determined using commercially available detection kits (F,G). *OLR1* mRNA expression was measured by RT-qPCR, while LOX-1 protein expression was analyzed by Western blotting (H,I). Data are represented as the mean  $\pm$  SD ( $n = 3$ ), with significance thresholds set at \* $p < 0.05$ , \*\* $p < 0.01$ , \*\*\* $p < 0.001$ .

### *BACH1 Was an m<sup>6</sup>A Regulatory Target of YTHDF1 in HCAECs*

BACH1 was identified as a downstream m<sup>6</sup>A-modified transcript regulated by YTHDF1 in HCAECs. As a central modulator of oxidative stress responses, BACH1 has been extensively implicated in the pathogenesis of cardiovascular diseases [19]. Bioinformatic analysis using the SRAMP platform predicted several putative m<sup>6</sup>A modification sites within the BACH1 mRNA sequence (Fig. 4A). Consistently, exposure to ox-LDL markedly elevated the m<sup>6</sup>A methylation level of BACH1 mRNA in HCAECs (Fig. 4B;  $p < 0.05$ ). Ox-LDL markedly increased BACH1 expression in HCAECs, whereas YTHDF1 knockdown significantly reduced BACH1 protein levels in ox-LDL-treated cells without affecting BACH1 mRNA expression (Fig. 4C,D;  $p < 0.05$ ). RIP assay result showed that YTHDF1 directly interacted with BACH1 (Fig. 4E). As demonstrated in Fig. 4F, pcDNA3.1-YTHDF1 transfection

significantly elevated YTHDF1 mRNA level in HCAECs ( $p < 0.05$ ). In addition, YTHDF1 overexpression significantly increased BACH1 protein level in HCAECs but did not affect BACH1 mRNA level, while m<sup>6</sup>A modification inhibitor (3-deazaadenosine; DAA) treatment significantly reduced BACH1 mRNA and protein levels in pcDNA.1-YTHDF1-transfected HCAECs (Fig. 4G,H;  $p < 0.05$ ). In summary, YTHDF1 promoted BACH1 mRNA translation in HCAECs in an m<sup>6</sup>A-dependent manner.

### *BACH1 Overexpression Reversed the Protective Roles of YTHDF1 Silencing on HCAECs Survival and Migration*

To investigate the interaction between YTHDF1 and BACH1 in regulating HCAECs' function, both BACH1 overexpression and YTHDF1 knockdown were induced, followed by exposure to ox-LDL stimulation. The transfection efficiency of pcDNA3.1-BACH1 was shown in Fig. 5A,B, demonstrating that pcDNA3.1-BACH1

markedly increased expression in HCAECs ( $p < 0.05$ ). As demonstrated in Fig. 5C, compared to the ox-LDL+shNC group, YTHDF1 downregulation did not affect the mRNA expression of BACH1, and co-transfection of pcDNA3.1-BACH1 greatly elevated BACH1 expression ( $p < 0.05$ ). Functional experiments subsequently showed that the promoting effects of YTHDF1 knockdown on ox-LDL-treated HCAEC viability and migration, as well as its inhibitory effect on cell apoptosis, were reversed by pcDNA3.1-BACH1 co-transfection (Fig. 5D–F;  $p < 0.05$ ). Moreover, the inhibitory role of YTHDF1 silencing on Cleaved-caspase-3/caspase-3 ratio and the promoting effect on p-eNOS and NO levels were reversed by BACH1 co-overexpression (Fig. 5G,H;  $p < 0.05$ ). To further support this observation, we conducted complementary experiments in which both BACH1 knockdown and YTHDF1 overexpression were induced in HCAECs, followed by ox-LDL treatment. The transfection efficiency of sh-BACH1 was shown in **Supplementary Fig. 1A**, and the results showed that sh-BACH1 transfection significantly reduced BACH1 mRNA level in HCAECs ( $p < 0.05$ ). It was subsequently observed that sh-BACH1 transfection significantly reduced BACH1 mRNA level in ox-LDL-treated HCAECs, while subsequent YTHDF1 overexpression only partially reversed this effect (**Supplementary Fig. 1B**;  $p < 0.05$ ). Functional experiments displayed that the promoting effects of BACH1 knockdown on ox-LDL-treated HCAEC viability and migration, as well as its inhibitory effect on cell apoptosis, were partially reversed by pcDNA3.1-YTHDF1 co-transfection (**Supplementary Fig. 1C–E**;  $p < 0.05$ ). Additionally, the inhibitory role of BACH1 silencing on Cleaved-caspase-3/caspase-3 ratio and the promoting effect on p-eNOS and NO levels were reversed by YTHDF1 co-overexpression (**Supplementary Fig. 1F,G**;  $p < 0.05$ ). In conclusion, YTHDF1 knockdown relieved ox-LDL-impaired HCAEC survival and migration by targeting BACH1.

#### *BACH1 Overexpression Diminished the Promoting Roles of YTHDF1 Knockdown on ox-LDL-Triggered Oxidative Stress and Inflammation in HCAECs*

The interaction between YTHDF1 and BACH1 in regulating endothelial oxidative stress and inflammation was subsequently investigated. As demonstrated in Fig. 6A–D, BACH1 overexpression prevented the sh-YTHDF1-induced decrease in TNF- $\alpha$ , IL-18, IL-1 $\beta$ , and VCAM-1 secretion levels in ox-LDL-treated HCAECs ( $p < 0.05$ ). Additionally, the inhibitory effects of YTHDF1 knockdown on ROS and MDA levels in ox-LDL-treated HCAECs, as well as its promoting effect on GSH level, were reversed by pcDNA3.1-BACH1 co-transfection (Fig. 6E–G;  $p < 0.05$ ). Moreover, BACH1 overexpression could effectively reverse the YTHDF1 silencing-induced suppression of LOX-1 expression (Fig. 6H,I;  $p < 0.05$ ). To further support this observation, we conducted complementary exper-

iments in which both BACH1 knockdown and YTHDF1 overexpression were induced in HCAECs, followed by ox-LDL treatment. The results showed that YTHDF1 overexpression partially prevented the sh-BACH1-induced decrease in TNF- $\alpha$ , IL-18, IL-1 $\beta$ , and VCAM-1 secretion levels in ox-LDL-treated HCAECs (**Supplementary Fig. 2A–D**;  $p < 0.05$ ). In addition, the inhibitory effects of BACH1 knockdown on ROS and MDA levels in ox-LDL-treated HCAECs, as well as its promoting effect on GSH level, were partially reversed by pcDNA3.1-YTHDF1 co-transfection (**Supplementary Fig. 2E–G**;  $p < 0.05$ ). Furthermore, YTHDF1 overexpression could partially reverse the BACH1 silencing-induced suppression of LOX-1 expression (**Supplementary Fig. 2H,I**;  $p < 0.05$ ). To sum up, YTHDF1 knockdown reduced ox-LDL-induced oxidative stress and inflammation in HCAECs by targeting BACH1.

## Discussion

CHD is a cardiovascular disease mainly caused by AS, which is characterized by a high incidence rate and mortality, usually leading to disability or even death [26,27]. As a central component of the vascular barrier, endothelial cells preserve vascular-wall homeostasis, sustain nonthrombotic blood–tissue interfaces, and actively shape immune responses [28]. Accordingly, impaired HCAEC function represents a key pathological driver of CHD [29]. Ox-LDL, a well-established atherosclerotic (AS) risk factor, encompasses LDL particles bearing heterogeneous oxidative alterations affecting both lipid moieties and apolipoprotein B [30]. Ox-LDL has a dual effect on HCAEC function. Specifically, low concentrations of ox-LDL can increase HCAEC proliferation, migration, and angiogenesis abilities; while high concentrations of ox-LDL in turn damage HCAEC cells, leading to endothelial dysfunction [31–33]. Due to the ongoing lack of clinically approved treatment plans for improving ox-LDL-induced HCAEC dysregulation, there is a pressing demand for novel approaches grounded in understanding underlying pathophysiological mechanisms. In this study, we observed that YTHDF1 expression was increased in PBMCs from patients with CHD and in ox-LDL-challenged HCAECs. Mechanistically, our data support that YTHDF1 silencing reduced ox-LDL-induced HCAEC dysregulation by reducing BACH1 expression level in an m<sup>6</sup>A-BACH1-dependent manner.

YTHDF1, a renowned m<sup>6</sup>A reader, participates in diverse biological processes, such as oxidative stress and inflammation. As proof, Zong *et al.* [34] revealed that YTHDF1 upregulation induced intestinal epithelial cell inflammatory injury and oxidative stress by promoting NLRP3 translation. In addition, YTHDF1 downregulation attenuated obesity-related vascular dysfunction and inflammation [35]. Notably, YTHDF1 upregulation promoted AS development by orchestrating inflammatory cascades in vascular endothelium [15]. However, the role

of YTHDF1 in regulating ox-LDL-induced HCAEC dysregulation is still unclear. Herein, our findings demonstrated that YTHDF1 was highly expressed in the PBMC samples of CHD patients and ox-LDL-treated HCAECs. Notably, given the significant between-group difference in HDL-C, we additionally adjusted for HDL-C as a covariate, and the upregulation of YTHDF1 in the CHD group remained significant, supporting that the observed association is not solely driven by dyslipidemia. In addition, YTHDF1 knockdown promoted ox-LDL-treated HCAEC survival and migration, and inhibited ox-LDL-induced oxidative stress and inflammation in HCAECs. Moreover, eNOS activation and subsequent NO production are essential for endothelial homeostasis, mediating vasodilation, anti-inflammatory effects, and anti-apoptotic functions, thus serving as critical markers of endothelial health [36]. ox-LDL is a well-documented disruptor of eNOS function, typically inducing its “uncoupling”—a state where the enzyme generates superoxide radicals instead of NO, exacerbating oxidative stress [37]. eNOS activity is tightly regulated through multiple mechanisms, with phosphorylation representing the most rapid and pivotal post-translational modification [38]. In our study, YTHDF1 silencing significantly enhanced eNOS phosphorylation at Ser1177, a key activation site. Collectively, these findings suggest that YTHDF1 inhibition may ameliorate ox-LDL-induced inflammation, oxidative stress, and endothelial dysfunction in an eNOS-dependent manner.

m<sup>6</sup>A, the prevalent mRNA modification, plays a pivotal role in epigenetic regulation of RNA processing, metabolism, and translation [39,40]. As an m<sup>6</sup>A reader, YTHDF1 recognizes and binds to m<sup>6</sup>A-modified motifs in mRNA, thereby promoting the translation of m<sup>6</sup>A-enriched mRNAs [41]. Herein, we investigated the m<sup>6</sup>A regulatory target of YTHDF1 in regulating ox-LDL-induced HCAEC dysregulation. BACH1 belongs to the alkaline leucine zipper protein family, which binds to small Maf proteins in the nucleus to form heterodimers. BACH1 functions in trans on AREs, inhibiting downstream target gene expression mediated by AREs and serving as a key effector of oxidative stress [42]. Our findings displayed that YTHDF1 facilitated BACH1 mRNA translation in HCAECs in an m<sup>6</sup>A-dependent manner. As widely described, BACH1 is closely related to endothelial cell function. Experimental evidence demonstrates that BACH1 exerts a suppressive effect on endothelial cell proliferation and migration, thereby compromising angiogenic capacity in a hind-limb ischemia model [43]. Mechanistically, BACH1 directly associates with the YAP promoter to enhance YAP transcription in endothelial cells, forming a BACH1–YAP regulatory complex that drives adhesion molecule expression and proinflammatory gene activation [19]. Furthermore, Rodrigues *et al.* [44] reported that BACH1 antagonizes Nrf2 by competing for DNA-binding sites, ultimately attenuating endothelial antioxidant defenses in patients with severe COVID-19. A

study on palmitate-induced endothelial dysfunction showed that cyanoglucose-3-O-glucoside treatment activated Nrf2 and reduced Bach1, induced Nrf2 nuclear translocation, and inhibited NF- $\kappa$ B signaling [18]. All the above evidence suggested that BACH1 was involved in regulating endothelial cells under CHD conditions. The present research revealed that BACH1 overexpression reversed the promoting effects of YTHDF1 knockdown on ox-LDL-treated HCAEC survival and migration and the inhibitory effects on ox-LDL-induced oxidative stress and inflammation. Collectively, YTHDF1 promoted ox-LDL-induced HCAEC dysregulation by enhancing BACH1 mRNA translation in an m<sup>6</sup>A-dependent manner.

LOX-1 is a type II integral membrane glycoprotein that was first identified in endothelial cells as the primary receptor for ox-LDL [45]. Extensive evidence indicates that LOX-1-mediated recognition of ox-LDL plays a central role in disrupting endothelial homeostasis and drives the progression of cardiovascular pathologies, including CHD [46,47]. Substantial evidence further highlights LOX-1’s pivotal role in mediating inflammatory responses and oxidative stress in cardiovascular diseases. For example, exercise intervention prevented the development of atherosclerosis by oxidative stress inhibition through inhibiting LOX-1 signaling [48]. In addition, LOX-1 inhibition has been shown to alleviate atherosclerosis by suppressing inflammation and reducing lipid deposition [49]. In the present research, ox-LDL treatment markedly upregulated *OLR1* mRNA and LOX-1 protein levels in HCAECs, whereas YTHDF1 silencing significantly attenuated this increase. Notably, BACH1 overexpression effectively reversed the suppressive effects of YTHDF1 knockdown on LOX-1 expression, suggesting that LOX-1 acts as a downstream effector of the YTHDF1/BACH1 axis in modulating endothelial function, inflammation, and oxidative stress. Despite these advances, the precise mechanistic link between YTHDF1/BACH1 and LOX-1 transcriptional regulation remains unexplored. Future studies will focus on elucidating whether YTHDF1-mediated m<sup>6</sup>A modification directly influences LOX-1 mRNA stability or translation and whether BACH1 binds to specific promoter/enhancer elements of the *OLR1* gene. These investigations will deepen our understanding of the epigenetic-metabolic crosstalk in endothelial injury and may identify novel therapeutic targets for CHD.

Although the *in vitro* nature of the current study, it provides meaningful insights for the research on the dysfunction of human coronary artery endothelial cells induced by ox-LDL. First, we used HCAECs, which are more representative of coronary pathophysiology than commonly used human umbilical vein endothelial cells (HUVECs) and human aortic endothelial cells (HAECs). Second, YTHDF1 upregulation in clinical CHD-derived PBMCs suggested its potential as a circulating biomarker. Third, we identified Bach1 as an m<sup>6</sup>A-dependent translational target of

YTHDF1 under ox-LDL stress, and linked this axis with endothelial cell survival, migration, inflammatory activation, oxidative stress and eNOS/NO signaling.

Despite these insights, several limitations should be acknowledged. All functional validations were performed *in vitro* using ox-LDL-induced HCAECs, which, while widely accepted, cannot fully replicate the complex microenvironment of *in vivo* atherosclerotic plaque formation. We did not systematically profile the dose–response or time–course effects of ox-LDL on YTHDF1 and BACH1 expression; therefore, our conclusions are confined to the commonly used injury condition (100 µg/mL, 48 h). Moreover, the lack of animal studies limits the direct extrapolation of our findings to systemic vascular pathophysiology. Due to limitations in research scope and experimental conditions, this study aims to establish a clear cellular-level regulatory framework. Future investigations using ApoE<sup>-/-</sup> mice will be essential to evaluate the impact of the YTHDF1/BACH1 axis on plaque development, endothelial function, and inflammatory infiltration *in vivo*. The impact of BACH1 on the expression of LOX-1 is an interesting finding, but the direct mechanism has not yet been elucidated. Further studies are warranted to explore the mechanism by which BACH1 regulates LOX-1 in ox-LDL-induced HCAEC dysfunction. YTHDF1 may regulate multiple m<sup>6</sup>A-modified mRNAs involved in endothelial dysfunction. This study only validated the mechanism by which YTHDF1 regulates BACH1, and other potential targets still need further identification and validation.

## Conclusion

Taken together, YTHDF1 knockdown alleviated HCAEC dysregulation during CHD progression by inhibiting BACH1 mRNA translation in an m<sup>6</sup>A-dependent manner. Our research provides a theoretical basis for developing novel treatment strategies for CHD.

## Abbreviations

CVD, Cardiovascular disease; CHD, Coronary heart disease; AS, Atherosclerosis; m<sup>6</sup>A, N<sup>6</sup>-methyladenosine; YTHDF1, YT521-B homology domain 1; HCAECs, Human coronary artery endothelial cells; BACH1, BTB and CNC homology 1; ox-LDL, Oxidized low-density lipoprotein; PBMCs, peripheral blood mononuclear cells; RT-qPCR, Reverse transcription quantitative polymerase chain reaction; CCK-8, Cell Counting Kit-8; ROS, Reactive oxygen species; ELISA, Enzyme-linked immunosorbent assay; TNF, Tumor necrosis factor; IL, Interleukin; VCAM-1, vascular cell adhesion molecule-1; NO, nitric oxide; eNOS, endothelial nitric oxide synthase; MDA, Malondialdehyde; GSH, Glutathione; DCFH-DA, 2',7'-dichlorodihydrofluorescein diacetate; HRP, horseradish peroxidase; MeRIP, Methylated RNA binding protein immunoprecipitation; RIP, RNA binding protein immunopre-

cipitation; SD, standard deviation; ANOVA, analysis of variance; ROC, receiver operating characteristic.

## Availability of Data and Materials

All data generated or analyzed are included in this article. Further inquiries can be directed to the corresponding author.

## Author Contributions

Conceptualization: LF; Methodology: JY; Formal Analysis: LF, RY, XC; Data curation: YY, MZ; Writing - Original Draft: LF; Writing - Review and Editing: all author; Resources: RY; Project administration: JY; Funding acquisition: JY; Investigation: LF; Supervision: JY. All authors have given final approval of the version to be published, agreed on the journal to which the article has been submitted, and agreed to be accountable for all aspects of the work.

## Ethics Approval and Consent to Participate

This study was approved by the Institutional Review Board of Fuwai Central China Cardiovascular Hospital (Approval No. 2025-102), and was performed in accordance with the Declaration of Helsinki. All participants provided the written informed consent.

## Acknowledgment

Not applicable.

## Funding

The study was supported by The Fund Project of Health Commission of Henan Province (Grant No. LHGJ20210121).

## Conflict of Interest

The authors declare no conflict of interest.

## Supplementary Material

Supplementary material associated with this article can be found, in the online version, at <https://doi.org/10.24976/Discov.Med.202638207.92>.

## References

- [1] Jokinen E. Coronary artery disease in patients with congenital heart defects. *Journal of Internal Medicine*. 2020; 288: 383–389. <https://doi.org/10.1111/joim.13080>.
- [2] Horio E, Kadomatsu T, Miyata K, Arai Y, Hosokawa K, Doi Y, *et al.* Role of endothelial cell-derived angptl2 in vascular inflammation leading to endothelial dysfunction and atherosclerosis progression. *Arteriosclerosis, Thrombosis, and Vascular Bi-*

- ology. 2014; 34: 790–800. <https://doi.org/10.1161/ATVBAHA.113.303116>.
- [3] Yazdani-Bakhsh R, Javanbakht M, Sadeghi M, Mashayekhi A, Ghaderi H, Rabiei K. Comparison of health-related quality of life after percutaneous coronary intervention and coronary artery bypass surgery. *ARYA Atherosclerosis*. 2016; 12: 124–131.
  - [4] Li Z, Song Y, Wang M, Shen R, Qin K, Zhang Y, *et al*. m6A regulator-mediated RNA methylation modification patterns are involved in immune microenvironment regulation of coronary heart disease. *Frontiers in Cardiovascular Medicine*. 2022; 9: 905737. <https://doi.org/10.3389/fcvm.2022.905737>.
  - [5] Jiang X, Liu B, Nie Z, Duan L, Xiong Q, Jin Z, *et al*. The role of m6A modification in the biological functions and diseases. *Signal Transduction and Targeted Therapy*. 2021; 6: 74. <https://doi.org/10.1038/s41392-020-00450-x>.
  - [6] Guo F, He M, Hu B, Li G. Levels and clinical significance of the m6A methyltransferase METTL14 in patients with coronary heart disease. *Frontiers in Cardiovascular Medicine*. 2023; 10: 1167132. <https://doi.org/10.3389/fcvm.2023.1167132>.
  - [7] Sun Y, Dong D, Xia Y, Hao L, Wang W, Zhao C. YTHDF1 promotes breast cancer cell growth, DNA damage repair and chemoresistance. *Cell Death & Disease*. 2022; 13: 230. <https://doi.org/10.1038/s41419-022-04672-5>.
  - [8] Jiang Y, Pan Y, Long T, Qi J, Liu J, Zhang M. Significance of RNA N6-methyladenosine regulators in the diagnosis and subtype classification of coronary heart disease using the Gene Expression Omnibus database. *Frontiers in Cardiovascular Medicine*. 2023; 10: 1185873. <https://doi.org/10.3389/fcvm.2023.1185873>.
  - [9] Yang X, Wang C, Zhu G, Guo Z, Fan L. METTL14/YTHDF1 axis-modified UCHL5 aggravates atherosclerosis by activating the NLRP3 inflammasome. *Experimental Cell Research*. 2023; 427: 113587. <https://doi.org/10.1016/j.yexcr.2023.113587>.
  - [10] Rajendran P, Rengarajan T, Thangavel J, Nishigaki Y, Sakthisekaran D, Sethi G, *et al*. The vascular endothelium and human diseases. *International Journal of Biological Sciences*. 2013; 9: 1057–1069. <https://doi.org/10.7150/ijbs.7502>.
  - [11] Kinlay S, Ganz P. Role of endothelial dysfunction in coronary artery disease and implications for therapy. *The American Journal of Cardiology*. 1997; 80: 11I–16I. [https://doi.org/10.1016/s0002-9149\(97\)00793-5](https://doi.org/10.1016/s0002-9149(97)00793-5).
  - [12] Drexler H, Hornig B. Endothelial dysfunction in human disease. *Journal of Molecular and Cellular Cardiology*. 1999; 31: 51–60. <https://doi.org/10.1006/jmcc.1998.0843>.
  - [13] Zhao F, Satyanarayana G, Zhang Z, Zhao J, Ma XL, Wang Y. Endothelial Autophagy in Coronary Microvascular Dysfunction and Cardiovascular Disease. *Cells*. 2022; 11: 2081. <https://doi.org/10.3390/cells11132081>.
  - [14] Wang F, Yang Q, Wang X, Guo Y, Lin S. CircYTHDF1/miR-19b-3p/YTHDF1 axis contributes to pregnancy-induced hypertension development by enhancing vascular endothelial cell injury. *Hypertension in Pregnancy*. 2024; 43: 2414976. <https://doi.org/10.1080/10641955.2024.2414976>.
  - [15] Chien CS, Li JYS, Chien Y, Wang ML, Yarmishyn AA, Tsai PH, *et al*. METTL3-dependent N<sup>6</sup>-methyladenosine RNA modification mediates the atherogenic inflammatory cascades in vascular endothelium. *Proceedings of the National Academy of Sciences of the United States of America*. 2021; 118: e2025070118. <https://doi.org/10.1073/pnas.2025070118>.
  - [16] Yin H, Ran Z, Luo T, Jin Z, Tan Y, Ma J. METTL3-YTHDF1 axis drives BCL-3 m6A methylation to promote the ferroptosis of brain microvascular endothelial cells during intracerebral hemorrhage. *Brain Research Bulletin*. 2025; 229: 111434. <https://doi.org/10.1016/j.brainresbull.2025.111434>.
  - [17] Zhang J, Wang C, Dong X. METTL14-mediated m6A methylation promotes macrophage M2 polarization via YTHDF1-Socs1 axis to accelerate skin wound healing. *European Journal of Medical Research*. 2025; 30: 813. <https://doi.org/10.1186/s40001-025-03056-7>.
  - [18] Fratantonio D, Speciale A, Ferrari D, Cristani M, Saija A, Cimino F. Palmitate-induced endothelial dysfunction is attenuated by cyanidin-3-O-glucoside through modulation of Nrf2/Bach1 and NF-κB pathways. *Toxicology Letters*. 2015; 239: 152–160. <https://doi.org/10.1016/j.toxlet.2015.09.020>.
  - [19] Jia M, Li Q, Guo J, Shi W, Zhu L, Huang Y, *et al*. Deletion of BACH1 Attenuates Atherosclerosis by Reducing Endothelial Inflammation. *Circulation Research*. 2022; 130: 1038–1055. <https://doi.org/10.1161/CIRCRESAHA.121.319540>.
  - [20] Yang Y, Wang Z, Xu Y, Liu X, Sun Y, Li W. Knockdown of lncRNA H19 alleviates ox-LDL-induced HCAECs inflammation and injury by mediating miR-20a-5p/HDAC4 axis. *Inflammation Research*. 2022; 71: 1109–1121. <https://doi.org/10.1007/s00011-022-01604-z>.
  - [21] Zhang Y, Li JJ, Xu R, Wang XP, Zhao XY, Fang Y, *et al*. Nogo-B mediates endothelial oxidative stress and inflammation to promote coronary atherosclerosis in pressure-overloaded mouse hearts. *Redox Biology*. 2023; 68: 102944. <https://doi.org/10.1016/j.redox.2023.102944>.
  - [22] Akhmedov A, Sawamura T, Chen CH, Kraler S, Vdovenko D, Lüscher TF. Lectin-like oxidized low-density lipoprotein receptor-1 (LOX-1): a crucial driver of atherosclerotic cardiovascular disease. *European Heart Journal*. 2021; 42: 1797–1807. <https://doi.org/10.1093/eurheartj/ehaa770>.
  - [23] Paquette M, Dufour R, Baass A. Scavenger Receptor LOX1 Genotype Predicts Coronary Artery Disease in Patients With Familial Hypercholesterolemia. *The Canadian Journal of Cardiology*. 2017; 33: 1312–1318. <https://doi.org/10.1016/j.cjca.2017.07.480>.
  - [24] Yan M, Mehta JL, Zhang W, Hu C. LOX-1, oxidative stress and inflammation: a novel mechanism for diabetic cardiovascular complications. *Cardiovascular Drugs and Therapy*. 2011; 25: 451–459. <https://doi.org/10.1007/s10557-011-6342-4>.
  - [25] Ying W, Meiyang S, Wen C, Kaizu X, Meifang W, Liming L. Liraglutide ameliorates oxidized LDL-induced endothelial dysfunction by GLP-1R-dependent downregulation of LOX-1-mediated oxidative stress and inflammation. *Redox Report: Communications in Free Radical Research*. 2023; 28: 2218684. <https://doi.org/10.1080/13510002.2023.2218684>.
  - [26] Kodama S, Saito K, Tanaka S, Maki M, Yachi Y, Asumi M, *et al*. Cardiorespiratory fitness as a quantitative predictor of all-cause mortality and cardiovascular events in healthy men and women: a meta-analysis. *JAMA*. 2009; 301: 2024–2035. <https://doi.org/10.1001/jama.2009.681>.
  - [27] Ren H, Wan X, Wei C, Yang G. Spatiotemporal variations in cardiovascular disease mortality in China from 1991 to 2009. *BMC Cardiovascular Disorders*. 2019; 19: 159. <https://doi.org/10.1186/s12872-019-1128-x>.
  - [28] Maier JAM, Malpuech-Brugère C, Zimowska W, Rayssiguier Y, Mazur A. Low magnesium promotes endothelial cell dysfunction: implications for atherosclerosis, inflammation and thrombosis. *Biochimica et Biophysica Acta*. 2004; 1689: 13–21. <https://doi.org/10.1016/j.bbadis.2004.01.002>.
  - [29] Zhou T, Li S, Yang L, Xiang D. microRNA-363-3p reduces endothelial cell inflammatory responses in coronary heart disease via inactivation of the NOX4-dependent p38 MAPK axis. *Aging*. 2021; 13: 11061–11082. <https://doi.org/10.18632/aging.202721>.
  - [30] Summerhill VI, Grechko AV, Yet SF, Sobenin IA, Orekhov AN. The Atherogenic Role of Circulating Modified Lipids in Atherosclerosis. *International Journal of Molecular Sciences*. 2019; 20: 3561. <https://doi.org/10.3390/ijms20143561>.
  - [31] Thum T, Borlak J. LOX-1 receptor blockade abrogates oxLDL-

- induced oxidative DNA damage and prevents activation of the transcriptional repressor Oct-1 in human coronary arterial endothelium. *The Journal of Biological Chemistry*. 2008; 283: 19456–19464. <https://doi.org/10.1074/jbc.M708309200>.
- [32] Tang F, Zhang S, Wang H, Xu S, Yang S, Zhu X, *et al*. lncRNA H19 Promotes Ox-LDL-Induced Dysfunction of Human Aortic Endothelial Cells through the miR-152/VEGFA Axis. *Journal of Healthcare Engineering*. 2022; 2022: 3795060. <https://doi.org/10.1155/2022/3795060>.
- [33] Ye F, Liu D, Zhang J. Transient receptor potential channel TRPM4 favors oxidized low-density lipoprotein-induced coronary endothelial cell dysfunction via a mechanism involving ferroptosis. *Tissue & Cell*. 2024; 86: 102290. <https://doi.org/10.1016/j.tice.2023.102290>.
- [34] Zong X, Xiao X, Jie F, Cheng Y, Jin M, Yin Y, *et al*. YTHDF1 promotes NLRP3 translation to induce intestinal epithelial cell inflammatory injury during endotoxic shock. *Science China. Life Sciences*. 2021; 64: 1988–1991. <https://doi.org/10.1007/s11427-020-1909-6>.
- [35] Shi XD, Zhang JX, Hu XD, Zhuang T, Lu N, Ruan CC. Leonurine Attenuates Obesity-Related Vascular Dysfunction and Inflammation. *Antioxidants (Basel, Switzerland)*. 2022; 11: 1338. <https://doi.org/10.3390/antiox11071338>.
- [36] Heiss C, Rodriguez-Mateos A, Kelm M. Central role of eNOS in the maintenance of endothelial homeostasis. *Antioxidants & Redox Signaling*. 2015; 22: 1230–1242. <https://doi.org/10.1089/ars.2014.6158>.
- [37] Yao Y, Wang Y, Zhang Y, Liu C. Klotho ameliorates oxidized low density lipoprotein (ox-LDL)-induced oxidative stress via regulating LOX-1 and PI3K/Akt/eNOS pathways. *Lipids in Health and Disease*. 2017; 16: 77. <https://doi.org/10.1186/s12944-017-0447-0>.
- [38] Kolluru GK, Siamwala JH, Chatterjee S. eNOS phosphorylation in health and disease. *Biochimie*. 2010; 92: 1186–1198. <https://doi.org/10.1016/j.biochi.2010.03.020>.
- [39] Wang X, Zhao BS, Roundtree IA, Lu Z, Han D, Ma H, *et al*. N(6)-methyladenosine Modulates Messenger RNA Translation Efficiency. *Cell*. 2015; 161: 1388–1399. <https://doi.org/10.1016/j.cell.2015.05.014>.
- [40] Liu ZX, Li LM, Sun HL, Liu SM. Link Between m6A Modification and Cancers. *Frontiers in Bioengineering and Biotechnology*. 2018; 6: 89. <https://doi.org/10.3389/fbioe.2018.00089>.
- [41] Hao WY, Lou Y, Hu GY, Qian CY, Liang WR, Zhao J, *et al*. RNA m6A reader YTHDF1 facilitates inflammation via enhancing NLRP3 translation. *Biochemical and Biophysical Research Communications*. 2022; 616: 76–81. <https://doi.org/10.1016/j.bbrc.2022.05.076>.
- [42] NandyMazumdar M, Paranjapye A, Browne J, Yin S, Leir SH, Harris A. BACH1, the master regulator of oxidative stress, has a dual effect on CFTR expression. *The Biochemical Journal*. 2021; 478: 3741–3756. <https://doi.org/10.1042/BCJ20210252>.
- [43] Jiang L, Yin M, Xu J, Jia M, Sun S, Wang X, *et al*. The Transcription Factor Bach1 Suppresses the Developmental Angiogenesis of Zebrafish. *Oxidative Medicine and Cellular Longevity*. 2017; 2017: 2143875. <https://doi.org/10.1155/2017/2143875>.
- [44] Rodrigues D, Machado MR, Alves JV, Fraga-Silva TFC, Martins RB, Campos LCB, *et al*. Cytokine storm in individuals with severe COVID-19 decreases endothelial cell antioxidant defense via downregulation of the Nrf2 transcriptional factor. *American Journal of Physiology. Heart and Circulatory Physiology*. 2023; 325: H252–H263. <https://doi.org/10.1152/ajpheart.00096.2023>.
- [45] Sawamura T, Kume N, Aoyama T, Moriwaki H, Hoshikawa H, Aiba Y, *et al*. An endothelial receptor for oxidized low-density lipoprotein. *Nature*. 1997; 386: 73–77. <https://doi.org/10.1038/386073a0>.
- [46] Pirillo A, Norata GD, Catapano AL. LOX-1, OxLDL, and atherosclerosis. *Mediators of Inflammation*. 2013; 2013: 152786. <https://doi.org/10.1155/2013/152786>.
- [47] Jin P, Cong S. LOX-1 and atherosclerotic-related diseases. *Clinica Chimica Acta; International Journal of Clinical Chemistry*. 2019; 491: 24–29. <https://doi.org/10.1016/j.cca.2019.01.006>.
- [48] Chan SH, Hung CH, Shih JY, Chu PM, Cheng YH, Lin HC, *et al*. Exercise intervention attenuates hyperhomocysteinemia-induced aortic endothelial oxidative injury by regulating SIRT1 through mitigating NADPH oxidase/LOX-1 signaling. *Redox Biology*. 2018; 14: 116–125. <https://doi.org/10.1016/j.redox.2017.08.016>.
- [49] Si Y, Du H, Li S, Zhang C, Wang J, Wang S, *et al*. Nitrate-driven maintenance of lipid homeostasis by M2 macrophages alleviates atherosclerosis via downregulation of LOX1 expression and reduction of lipid deposition. *Science China. Life Sciences*. 2025; 68: 2995–3009. <https://doi.org/10.1007/s11427-025-3020-2>.